# Role of the shell thickness in stimulated emission and photoinduced absorption in CdSe core/shell nanorods

Arianna Cretí,[1,*] Margherita Zavelani-Rossi,[1] Guglielmo Lanzani,[1] Marco Anni,[2] Liberato Manna,[3] and Mauro Lomascolo[4]
[1]*National Laboratory for Ultrafast and Ultraintense Optical Science ULTRAS-CNR-INFM, Dipartimento di Fisica, Politecnico di Milano, Piazza L. Da Vinci 32, 20133 Milano, Italy*
[2]*NNL National Nanotechnology Laboratory of INFM and Dipartimento di Ingegneria dell'Innovazione, Universitá degli Studi di Lecce, Via per Arnesano, I-73100 Lecce, Italy*
[3]*NNL National Nanotechnology Laboratory of INFM, Università degli Studi di Lecce, Via per Arnesano, I-73100 Lecce, Italy*
[4]*IMM-CNR, Istituto per la Microelettronica e Microsistemi, Campus Universitario, Strada Provinciale per Monteroni, I-73100 Lecce, Italy*

(Received 5 December 2005; revised manuscript received 7 March 2006; published 13 April 2006)

The effect of the shell thickness on stimulated emission and photoinduced absorption transitions in CdSe quantum rods is investigated by femtosecond pump and probe spectroscopy. The role of surface/interface defect states, which result resonant to the high energy states and to the midgap, respectively, is pointed out. We find that the density of such states depend on the shell thickness and that the interface defects can be negligible for thin shells. As a result in the latter case stimulated emission can be observed for longer times.

DOI: 10.1103/PhysRevB.73.165410 PACS number(s): 78.47.+p, 78.67.Bf, 73.22.−f, 71.55.−i

Strong interest in colloidal semiconductor nanocrystals (NC) arises from their unique electronic and optical properties, that can be controlled by their shapes and their sizes. Nowadays quantum dots (QDs),[1] quantum rods (QRs),[2] and tetrapods NC (Ref. 3) are very promising for biological labels[4] and optoelectronic devices.[5] Tunable amplified spontaneous emission (ASE) and optical gain have been also achieved[6–8] in colloidal QDs and QRs.

To fully exploit NC potentialities one should know in detail the electronic structure and its relationship to their composition. It has been recently demonstrated that surface states strongly affect the photoinduced processes of NC.[9,10] Overgrowing the NC with a shell of a higher band-gap semiconductor improves the photoluminescence (PL) quantum yield (QY) and the stability[1] and this improvemement depends on the shell thickness.[11] In fact, the strain relaxation at the interface introduces new extended defects[1,12] that change NC optical properties. Electron microscopy observations give evidence of misfit dislocations in such core/shell (CS) structures.[13] Very recently we have clarified the role of the surface and interface defects on the competition between stimulated emission (SE) and photoinduced absorption (PA) processes in CdSe core and core/shell nanorods.[10] In particular we demonstrated that in core quantum rods the bare surface defects are resonant to the high energy intrinsic levels and they can be passivated by the shell. However, the shell can introduce new defects which are resonant to the midgap. As a result the shell reduces carrier trapping from high energy defects and increases the PL QY, but causes new PA processes from midgap defects states that compete with SE. These results demonstrate that the improvement of both the QR quantum yield and the optical gain requires an effective passivation of the high energy surface states without the introduction of low energy defect states. As the last states are probably due to surface strain relaxation, a thinner shell could be expected to ensure a good compromise between the two processes.

In this report we study the role of the shell in PA and SE processes, by comparing the core QR with core/shell QR with a thin shell (0.50 ML). The comparison of the obtained results with the one obtained in Ref. 10 for thick shell QR (0.80 ML) allows us to investigate the role of the shell thickness[14] on the QR photoinduced processes. We demonstrate that, despite the similar confinement in the core, thin shell and thick shell samples, strong differences in the photoinduced properties are present, that are attributed to the different distribution of defect states. In particular we show that the thin shell partially saturates the surface states, thus allowing us to increase the QY of about one order of magnitude, without introducing low energy states competing with SE.

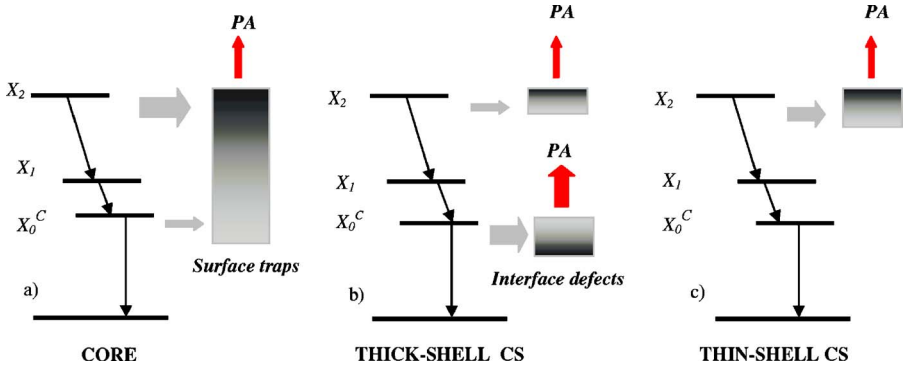


FIG. 1. (Color online) Energy level diagram for (a) the core sample, (b) the thick-shell CS sample, and (c) the thin-shell CS sample.

 

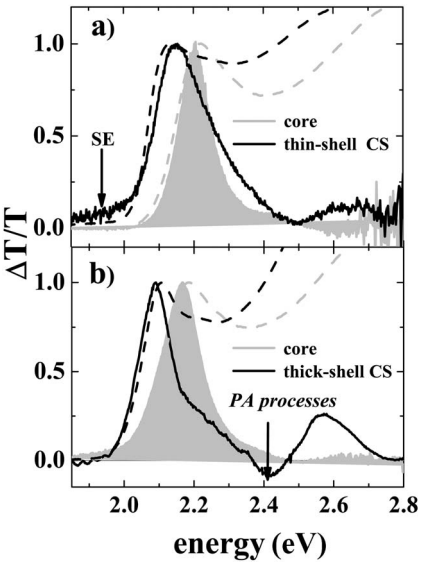


FIG. 2. $\Delta T/T$ differential transmission spectra recorded 4 ps after excitation (continuous lines), with an excitation fluence of 160 $\mu$J/cm$^2$ at 3.18 eV for (a) core and thin-shell CS and (b) core and thick shell CS sample (the latter investigated in Ref. 10). The linear absorption spectra are also shown for each sample (dashed lines).

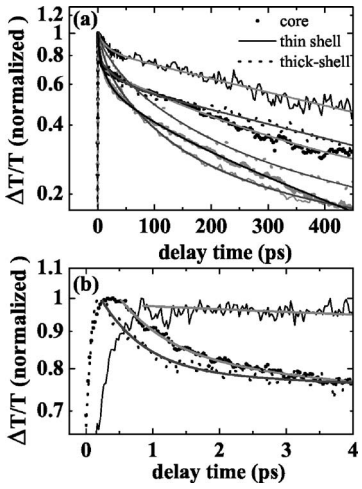


FIG. 3. (a) Bleaching $\Delta T/T$ kinetics recorded at the $X_0$ band of core and thin-shell CS samples at an excitation fluence of 160 $\mu$J/cm$^2$ (grey symbols and line) and 16 $\mu$J/cm$^2$ (dark symbols and line) and of thick-shell CS sample at an excitation fluence of 160 $\mu$J/cm$^2$ (grey dotted line) and 50 $\mu$J/cm$^2$ (dark dotted line) together with multiexponential best fits. (b) Zoom in the first 4 ps at the lower excitation fluence.

These effects allow to considerably increase the SE lifetime with respect to both the core and the thick shell CS QR. In Fig. 1 schematic energy level diagrams including the defect states are shown for core and the thick-shell CS nanorods[10] and the one expected for thin-shell CS rods.

Core CdSe and CdSe/CdS/ZnS CS nanorods were prepared following the procedure described in Ref. 15. We used cores with diameter of 3.5 nm and length of 22 and 29 nm,[10] on average, with a size dispersion of 14% and cores covered with a 0.50 and 0.80 ML (Ref. 10) shell which increases the QY by one order of magnitude up to 4%.

The laser excitation source was the second harmonic (390 nm, 3.18 eV) of an amplified Ti:sapphire laser which provides 150-fs, 750-$\mu$J pulses at 780 nm at 1-kHz repetition rate. Transient transmission changes $\Delta T$ were measured by pump and probe experiments carried out using the white light supercontinuum generated in a 2-mm-thick sapphire plate as the probe beam. Mirrors were used for the supercontinuum to minimize frequency chirp effects. The pump beam was linearly polarized at the magic angle (54.7°) with respect to the probe. Normalized $\Delta T/T$ spectra were recorded by an optical multichannel analyzer and the temporal evolution of $\Delta T/T$ were recorded using standard lock-in technique and 10-nm bandwidth interference filters. All experiments were performed with nanorods dispersed in chloroform solution and at room temperature.

Figure 2 displays normalized chirp-free differential transmission $\Delta T/T$ spectra of (a) the thin-shell CS and of (b) the thick-shell CS QRs (Ref. 10) together with the spectra of the corresponding core QRs. The pump and probe delay is 4 ps and the excitation fluence 160 $\mu$J/cm$^2$. The linear absorption spectra are also shown for comparison (dashed lines). In $\Delta T/T$ spectra bleaching and SE give positive signals, while negative signals arise from PA processes involving exciton states or defect states. In our samples the exciton levels are basically the same because the QRs have the same diameter. The different lengths do not strongly modify the confinement energy[16] so differences in $\Delta T/T$ spectra have to be ascribed to differences in the defects distribution or density, which give rise to different PA transitions.

At energies higher than the first exciton transition $X_0$, we observe that the $\Delta T/T$ are due to the overlap of absorption bleaching and of PA signal that decreases the bleaching signal with respect to the expected one (by looking at the absorption spectra). In particular the core $\Delta T/T$ spectrum shows a negative band at about 2.6 eV. This PA band can be attributed to surface states photoinduced absorption.[10] When the thin shell is present the $\Delta T/T$ signal at about 2.6 eV

TABLE I. Decay times in picoseconds for core sample bleaching. $X_0$ correspond to 2.21 eV, $X_1$ to 2.43 eV, and $X_2$ to 2.58 eV. $N_0$ in QRs on average is 2.5, except for data in the last row.

| | $\tau_{rise}$ | $\tau_1$ | $\tau_2$ | $\tau_3$ | $\tau_4$ |
|---|---|---|---|---|---|
| $X_0$ | 0.460±0.030 | 1.2±0.05 | 13±1.0 | 79±15 | 448±24 |
| $X_1$ | 0.300±0.030 | 0.5±0.2 | 7.5±0.1 | 74±2 | 500±15 |
| $X_2$ | 0.190±0.030 | 0.360±0.001 | 17±10 | 42±10 | 500±100 |
| $X_0(N_0=0.3)$ | 0.300±0.040 | 0.9±0.03 | 9.5±1.0 | | 390±5 |

TABLE II. Decay times in picoseconds for thin-shell CS sample. $X_0$ correspond to 2.14 eV, $X_1$ to 2.38 eV, and $X_2$ to 2.63 eV. $N_0$ in QRs on average is 2.5, except for data in the last row.

| | $\tau_{rise}$ | $\tau_1$ | $\tau_2$ | $\tau_3$ | $\tau_4$ |
|---|---|---|---|---|---|
| $X_0$ | 0.950±0.030 | | 10.0±1.0 | 74±3 | 810±70 |
| $X_1$ | 0.360±0.030 | 1.00±0.05 | 10.0±0.5 | 63±9 | 613±38 |
| $X_2$ | 0.240±0.030 | 0.40±0.01 | 8.5±0.5 | 63±12 | 640±40 |
| $X_0(N_0=0.3)$ | 0.350±0.008 | | 12.0±2 | | 687±9 |

becomes positive, due to the PA reduction. It is interesting to observe that the 2.6 eV signal in thin shell samples is smaller than the one visible in thick shell rods [see Fig. 2(b)], suggesting an only partial saturation of the surface defects. Moreover the thin shell overgrowth leads to a $\Delta T/T$ positive signal in the emission region of the sample, that can be attributed to SE. This suggests that the low energy defect states, competing with SE in thick shell samples, are not present in the thin shell ones. Moreover the SE is not evident in the low energy region of the short core samples [Fig. 2(a)] while it is present in the longer ones [Fig. 2(b)]. This can be ascribed to Auger relaxation processes which are higher in shorter NCs due to higher confinement.[17]

In order to determine the role and the energy distribution of defects we performed time-resolved differential transmission $\Delta T/T$ measurements at probe energies corresponding to the exciton transitions $X_0$, $X_1$ and $X_2$ (see Tables caption), and at lower energies where SE is expected.

Bleaching signals at $X_0$, $X_1$, and $X_2$ can be fitted with multi-exponential decays. In Fig. 3 are shown, as an example, the data for $X_0$ in the core, thin-shell, and thick-shell CS samples. In Tables I–III we report the best fit decay constants and the rise times for the same QRs. The rise time is defined as the time interval from the 10% to the 90% of the rising signal. With a pump fluence of 160 $\mu J/cm^2$ the average number of electron-hole pairs excited was $N_0=2.5$ in shorter QRs and $N_0=3.5$ in the longer ones.

In all samples we observe in the first picosecond the same cascading phenomenon of excited carriers from higher levels to lower ones: $X_2$ is immediately populated (within the time resolution of the experiment), then rapid intraband relaxation occurs by intrinsic thermalization processes from $X_2$ to $X_1$ and from $X_1$ to $X_0$ band, as we can deduce by the comparison between the fastest decay time and the rise time of the corresponding lower energy band. On the contrary, the lower exciton level $X_0$ shows a different behavior in core and core/shell samples. In fact a rapid decay time (of about 1 ps) is observed in core sample signal and it is attributed to trapping in defect states, located at the core surface. A thin shell passivates them, moreover it does not introduce new defects in the midgap, in contrast to the thick shell where these new defects are responsible for the fastest relaxation process also observed in $X_0$.

The role of trapping mechanism can be further evidenced by measuring differential transmission dynamics at different pump fluences. The pump fluence dependence of the $X_0$ bleaching dynamics is reported in Fig. 3(a). The best fit decay times (see Tables I–III) show that in the core sample and in the thick-shell CS samples the decay time $\tau_1$ increases as the pump fluences increases, due to saturation of defects.

In the core and thin-shell core/shell samples a new fast decay process with decay time $\tau_3$ is observed at high excitation fluences, and it is attributed to Auger recombination.[17] In the thick-shell sample we observe that $\tau_3$ becomes faster at high excitation fluences, also in agreement with the fluence dependence of the Auger process. Note also that the Auger recombination processes are faster in shorter rods with respect to the longer rods, even though the population of excited carriers is reduced (2.5 vs 3.5), as expected from the higher confinement.[17] The other time constants do not depend on the pump fluence.

SE was measured at 2.03 eV for the core and at 1.98 eV for the thin-shell CS sample. The traces are shown in Fig. 4. These dynamics show a photoinduced absorption in the first 700 fs, involving defect states, and then a positive signal. The PA signal in thin-shell sample is smaller than the one observed in core QRs. This confirms the reduction of the trapping from highly excited states due to the shell growth. The positive signal can be fitted with a biexponential decay. The decay time constants are similar to the bleaching ones $\tau_2$ and $\tau_3$ in both samples. This matching suggests that the relaxation processes involved in both signals are the relaxation from the emitting exciton state ($\tau_2$) and the Auger recombination process ($\tau_3$). We observe that in both samples the strong Auger recombination prevents to observe in the SE signal the typical long radiative lifetime of about 1 ns in these structures.[18]

The $\tau_4$ bleaching lifetime is instead attributed to relaxation from the defect states. This decay time is in fact not observed in the SE dynamics (thus ruling out a relaxation process of the emitting states) and is in agreement with the lifetime of the PA at low probe energy (1.90 eV and 1.98 eV) in the core sample (not shown).

Finally we have determined the upper limit for gain lifetime, by determining how long the SE signal is stronger than

TABLE III. Decay times in picoseconds for thick-shell CS sample. $X_0$ correspond to 2.10 eV, $X_1$ to 2.29 eV, and $X_2$ to 2.58 eV. $N_0$ in QRs on average is 3.5, except for data in the last row.

| | $\tau_{rise}$ | $\tau_1$ | $\tau_2$ | $\tau_3$ | $\tau_4$ |
|---|---|---|---|---|---|
| $X_0$ | 0.990±0.030 | 9±1 | 27±10 | 122±10 | 565±20 |
| $X_1$ | 0.530±0.030 | 0.82±0.05 | 17±5 | 100±10 | 550±20 |
| $X_2$ | 0.280±0.015 | 0.487±0.014 | 22±5 | 120±10 | 550±20 |
| $X_0(N_0=0.8)$ | 0.280±0.020 | 0.60±0.03 | 28.0±10 | 200±50 | 660±100 |

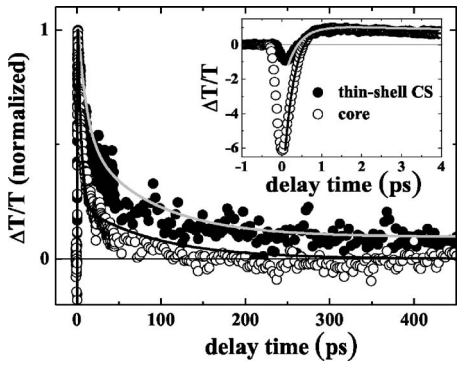


FIG. 4. Time evolution of the SE for the core and thin-shell CS samples, recorded at 2.03 eV and 1.98 eV respectively. Inset: zoom in the first 4 ps.

the PA one, after the pump pulse, by considering the ratio between $\Delta T/T$ in the SE region and at $X_0$ and the ratio between linear absorption in the region of SE and linear absorption at $X_0$. As far as the first ratio is higher than the second one SE is stronger than PA.[10] Figure 5 shows these data. SE is achieved in core, thin-shell and thick-shell CS samples (at 1.88 eV), but it is longer living in the thin-shell sample (~150 ps vs 40 ps of the core sample). Moreover in thin shell the SE lifetime is strongly increased with respect to thick-shell CS QRs, characterized by a very short living SE (25 ps) due to defects which trap the carriers below the absorption onset, resonant to the lowest energy emitting states. So it appears that the thin shell enhances SE processes, with respect to bare cores or thick-shell CS QRs, because it reduces defects that trap excited carriers and cause photoinduced absorption which can compete with SE.

In conclusion we demonstrated that SE strongly depends on the energy distribution of defects states in NCs, namely, depends on the presence and on the thickness of the shell. In

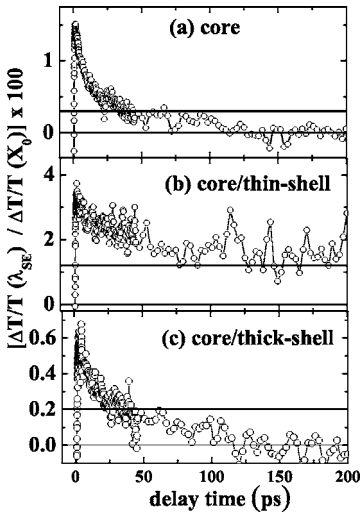


FIG. 5. Time evolution of the SE (more details in the text) for the (a) core, (b) thin-shell CS samples, and (c) thick-shell CS samples. The continuous lines represent the SE threshold resulting from linear absorption spectrum for each sample.

particular in core QRs the defect states are prevalently distributed resonantly to the higher exciton states. When QRs are coated the density of these high energy defects is reduced and the reduction is more efficient for thicker shells. However, thick shells introduce new defect states at the midgap, due to strain relaxation at the core-shell interface. The defects density is higher for thick shells, while it becomes negligible reducing the shell thickness. These conclusions explain the increase of PL QY and the decrease of PA from high energy levels in both, thick and thin core/shell QRs, compared to core samples, and the increase of SE only in thin-shell CS QRs.

*Also at ISUFI Institute for advanced interdisciplinary studies, Universitá degli Studi di Lecce, Via per Arnesano, 73100 Lecce, Italy; Electronic address: arianna.creti@le.imm.cnr.it

[1] B. O. Dabbousi, J. Redriguez-Vejo, F. V. Mikulec, J. R. Heine, H. Mattousi, R. Ober, K. F. Jensen, and M. G. Bawendi, J. Phys. Chem. B **101**, 9463 (1997), and references therein.
[2] J. Hu, L. Li, W. Yang, L. Manna, L. Wang, and A. P. Alivisatos, Science **292**, 2060 (2001).
[3] L. Manna, D. J. Milliron, A. Meisel, E. C. Scher, and A. P. Alivisatos, Nat. Mater. **2**, 382 (2003).
[4] A. P. Alivisatos, Nat. Biotechnol. **22**, 47 (2004).
[5] W. U. Huynh, J. J. Dittmer, and A. P. Alivisatos, Science **295**, 2425 (2002).
[6] A. Malko, A. A. Mikhailovsky, M. A. Petruska, J. A. Hollingsworth, H. Htoon, M. G. Bawendi, and V. I. Klimov, Appl. Phys. Lett. **81**, 1303 (2002).
[7] V. I. Klimov, A. A. Mikhailovsky, S. Xu, A. Malko, J. A. Hollingsworth, C. A. Leatherdale, H.-J. Eisler, and M. G. Bawendi, Science **290**, 314 (2000).
[8] M. Kazes, D. Y. Lewis, Y. Ebenstein, T. Mokari, and U. Banin, Adv. Mater. (Weinheim, Ger.) **14**, 317 (2002).
[9] A. V. Malko, A. A. Mikhailovsky, M. A. Petruska, J. A. Hollingsworth, and V. I. Klimov, J. Phys. Chem. B **108**, 5250 (2004).
[10] A. Cretí, M. Anni, M. Z. Rossi, G. Lanzani, G. Leo, F. D. Sala, L. Manna, and M. Lomascolo, Phys. Rev. B **72**, 125346 (2005).
[11] X. Chen, Y. Lou, A. C. Samia, and C. Burda, Nano Lett. **3**, 799 (2003).
[12] X. Peng, M. C. Schlamp, A. V. Kadavanich, and A. P. Alivisatos, J. Am. Chem. Soc. **119**, 7019 (1997).
[13] Y. W. Cao and U. Banin, J. Am. Chem. Soc. **122**, 9692 (2000).
[14] We observe that in both samples, on average, the shell does not form a complete monolayer. The shell average thickness increase in the "thick shell" samples is then not only due to a shell thickness increase, but also to an increased average shell surface coverage.
[15] L. Manna, E. C. Scher, and A. P. Alivisatos, J. Am. Chem. Soc. **122**, 12700 (2000).
[16] S. Kan, T. Mokari, E. Rothenberg, and U. Banin, Nat. Mater. **2**, 155 (2003).
[17] H. Htoon, J. A. Hollingsworth, R. Dickerson, and V. I. Klimov, Phys. Rev. Lett. **91**, 227401 (2003).
[18] X. Y. Wang, J. Y. Zhang, A. Nazzal, M. Darragh, and M. Xiao, Appl. Phys. Lett. **81**, 4829 (2002).